Calibration and Validation of *HY-2* Altimeter Wave Height

QINGXIANG LIU,*,+,# ALEXANDER V. BABANIN,# CHANGLONG GUAN,*,+
STEFAN ZIEGER,# JIAN SUN,*,+ AND YONGJUN JIA@

* *Physical Oceanography Laboratory, Ocean University of China, Qingdao, China*
+ *Qingdao Collaborative Innovation Center of Marine Science and Technology, Ocean University of China, Qingdao, China*
# *Faculty of Science, Engineering and Technology, Swinburne University of Technology, Melbourne, Victoria, Australia*
@ *National Satellite Ocean Application Service, State Oceanic Administration, Beijing, China*

(Manuscript received 2 November 2015, in final form 12 February 2016)

ABSTRACT

Hai Yang-2 (*HY-2*) satellite altimeter measurements of significant wave height (H_s) are analyzed over the period from 1 October 2011 to 6 December 2014. They are calibrated and validated against in situ buoys and other concurrently operating altimeters: *Jason-2*, *CryoSat-2*, and *Satellite with Argos and ALtiKa* (*SARAL*). In general, the *HY-2* altimeter measurements agree well with buoy measurements, with a bias of −0.22 m and a root-mean-square error (RMSE) of 0.30 m. When the reduced major axis (RMA) regression procedure was applied to the entire period, the RMSE was reduced by 33% to 0.2 m. A further comparison with other satellite altimeters, however, revealed two additional features of *HY-2* H_s estimates over this period. First, a noticeable mismatch is present between *HY-2* and the other satellite altimeters for high seas ($H_s > 6$ m). Second, a jump increase in *HY-2* H_s values was detected starting in April 2013, which was associated with the switch to backup status of the *HY-2* sensors and the subsequent update of its data processing software. Although reported by previous studies, these two deficiencies had not been accounted for in calibrations. Therefore, the *HY-2* wave height records are now subdivided into two phases (time periods pre- and post-April 2013) and a two-branched calibration is proposed for each phase. These revised calibrations, validated throughout the range of significant wave heights of 1–9 m, are expected to improve the practical applicability of *HY-2* H_s measurements significantly.

1. Introduction

Ocean surface winds and waves are of much interest to the oceanography and ocean engineering communities. They interact with each other in a very complicated manner. On the one hand, winds generate waves through the component of pressure in quadrature with the wavy surface (e.g., Young 1999). On the other hand, waves influence sea surface drag and consequently change the flux transferred by winds and the very winds that generated them (e.g., Janssen 2004; Babanin and Makin 2008). When waves propagate against local winds, wave decay is also expected (Donelan 1999). To investigate winds and waves, apart from building analytical theories and numerical models, in situ or remote sensing measurements of them is crucial. Among the diverse methods to observe winds and waves, satellite radar altimeters play a special role. Although having a limited time resolution when compared with buoys or other platforms, altimeters provide an excellent global coverage and by now satellite data have been available for three decades (e.g., Young et al. 2011, 2015). It is well known that the earliest global wave measurements by satellite altimetry can be dated back to 1985, when *Geosat* was launched (e.g., Zieger et al. 2009). So far, with the efforts of agencies from different countries, a total of 11 satellite altimeter missions have been operational, including the most recent ones by *Jason-2* (Dumont et al. 2011), *CryoSat-2* (ESRIN/MSSL 2012), *Satellite with Argos and ALtiKa* (*SARAL*; Bronner et al. 2013), and *Hai Yang-2* (*HY-2*; NSOAS 2013). *HY-2* (also termed *HY-2A*), launched on 16 August 2011, is China's first dynamic environmental satellite. It is positioned in a sun-synchronous orbit at an altitude of 971 km and an inclination of 99.34°. Its nodal period is 104.46 min, which translates into an exact repeat ground-track cycle of 14 days (see also Table 1). In addition to a radar altimeter,

Corresponding author address: Changlong Guan, Physical Oceanography Laboratory, Ocean University of China, 238 Songling Road, Qingdao 266100, China.
E-mail: clguan@ouc.edu.cn

DOI: 10.1175/JTECH-D-15-0219.1

TABLE 1. Summary of altimeter missions and data used in this paper including orbit parameters, data duration and source, and the percentage of flagged records, etc. Note that *CryoSat-2* here denotes its low-resolution, nadir-looking altimeter mode, and except for the repeat period of 369 days, it also has a subcycle period of 30 days.

Satellite	Inclination (°)	Repeat period (days)	Band	Data type	Duration	Source	Flagged records (%)
Jason-2	66.0	9.9	Ku	GDR-D	25 Sep 2011–19 Oct 2014	AVISO	19.9
CryoSat-2	92.0	369	Ku	IGDR	29 Sep 2011–4 Dec 2014	NOAA/NESDIS	14.6
HY-2	99.3	14	Ku	IGDR	1 Oct 2011–6 Dec 2014	NSOAS	21.6
SARAL	98.6	35	Ka	GDR-T	14 Mar 2013–30 Oct 2014	AVISO	13.9

HY-2 is also equipped with three other microwave sensors: a scatterometer, a scanning radiometer, and a calibration radiometer. This enables it to simultaneously monitor multiple ocean surface dynamic parameters, such as wind speed and direction, wave height, sea surface height, and temperature. Similar to *Jason-2*, the *HY-2* altimeter operates at dual-frequency bands: Ku band (13.58 GHz) and C band (5.25 GHz). Note that although *HY-2* was initially planned for 3 years of operation, at present it is still fully operational. To provide an uninterrupted ocean monitoring service, the Chinese National Satellite Ocean Application Service (NSOAS) has started developing follow-on satellite missions, namely, HY-2B and HY-2C, which are scheduled to launch in 2017 and 2018, respectively.

Retrieving the 10-m wind speed (U_{10}) and significant wave height (H_s) from satellite altimetry are fairly straightforward (Chelton et al. 2001). The altimeter transmits to the rough sea surface, a limited microwave pulse of known power P_t and receives it back after a certain time; this is termed as the two-way travel time t. Because of attenuation by the intervening atmosphere (dry air, water vapor, clouds, and rain, etc.) and the scattering characteristics of the sea surface, the received power P_r is less than P_t and the ratio of P_r/P_t can be represented by the so-called normalized radar cross section σ_0 (also termed backscatter). The time t is used to determine sea surface height h. Once various corrections have been taken into account, the accuracy of h can be improved to a few centimeters, which meets requirements for investigations of ocean currents. The slope of the leading edge of the returned signal is related to H_s: the higher the H_s, the lower the slope. Finally σ_0, which is related to the roughness of the ocean surface, is used for deriving U_{10}, usually through an empirical algorithm (e.g., Gourrion et al. 2002; Abdalla 2012). Unlike that of the scatterometer, the σ_0 of the altimeter decreases with increasing U_{10}. Because of the random nature of a wave field on an ocean surface, the noisy returned signals are always averaged and convoluted with other factors, such as the probability distribution function of the sea surface height, the shape of the transmitted pulse, and the altimeter antenna gain, to finalize a smooth returned waveform. A few tens of waveforms (e.g., 20 for *Jason-2* and 40 for *SARAL*) are further averaged to obtain the so-called 1-Hz records for practical applications.

Altimeter-derived 1-Hz U_{10} and H_s have been extensively used in the literature. As mentioned above, because of the excellent global coverage of altimeter-provided H_s measurements, they can be applied to tune and validate source term components in numerical wave models (e.g., Tolman 2002; Ardhuin et al. 2010; Zieger et al. 2015) and also to verify wave hindcast data archived in operational centers or institutes (e.g., Chawla et al. 2013; Rascle and Ardhuin 2013). Unlike wind observations provided by a scatterometer, the altimeter-derived U_{10} is not usually assimilated into atmospheric models. Therefore, as an independent database, it can be used to evaluate or intercompare different reanalyses (e.g., Caires et al. 2004; Stopa and Cheung 2014). Another advantage of altimeter wind and wave products is their continuity in time, which provides an extraordinary opportunity to study wind–wave climatologies and their trends (e.g., Young et al. 2011). Combined with U_{10} measured by altimeters or other platforms, altimeter-estimated H_s measurements can also find their way to generate global climatologies and seasonal patterns of wind seas and swell (Chen et al. 2002). In addition, Young et al. (2013) demonstrated that by considering certain altimeter transects in the Southern Ocean, a possibility of using altimeter-measured H_s to investigate the decay rate of oceanic swell, upon which these authors then proposed a source term pertaining to swell dissipation for wave models. Other possibilities for the application of satellite altimeter measurements range from assimilating H_s measurements into wave models (e.g., Lionello et al. 1992), monitoring the extreme sea states generated by extratropical and tropical storms (e.g., Tolman et al. 2005; Hanafin et al. 2012; Smith et al. 2013), and validating and optimizing parametric hurricane wave models (Young and Vinoth 2013). It is worth mentioning that additional parameters can also be inferred from a satellite altimeter, such as wave period (e.g., Gommenginger et al. 2003; Mackay et al. 2008; Badulin 2014), ice type (Tran et al. 2009; Rinne and Skourup

TABLE 2. Summary of previous studies on calibrating *HY-2* H_s data. The calibrations for Wang et al. (2013) and Ye et al. (2015) are inferred from their original formulas by inverse regression. All the studies used a buoy–altimeter collocation criteria of 30 min for temporal separation and 50 km (or approximate metrics, e.g., 0.5°) for spatial separation.

Study	Period	No.	Bias (m)	RMSE (m)	Calibration
Yang et al. (2014)	1 Oct 2011–30 Jun 2012	412	−0.30	0.38	$H_s^* = 1.070 \times H_s + 0.140$
Chen et al. (2013)	1 Dec 2011–31 May 2012	617	−0.22	0.36	$H_s^* = 1.077 \times H_s + 0.067$
Wang et al. (2013)	1 Oct 2011–29 Aug 2012	902	−0.17	0.30	$H_s^* = 1.122 \times H_s - 0.025$
Zhang et al. (2015)	1 Oct 2011–31 Dec 2013	1775	−0.23	0.34	$H_s^* = 1.031 \times H_s + 0.173$
Ye et al. (2015)	1 Oct 2011–30 Sep 2014	3745	−0.13	0.38	$H_s^* = 1.176 \times H_s - 0.200$

2012), and size (freeboard and area) of small icebergs (Tournadre et al. 2008). The latter two ice-related parameters can be further utilized to study wave climates (Zieger et al. 2013; Babanin et al. 2014) and to interpret the error source in numerical wave models (Ardhuin et al. 2011) in marginal ice zones.

To sum up, by covering long periods of time and extended spatial scales, altimeter-estimated U_{10} and H_s are reliable, useful, and therefore valuable. The uncorrected altimeter measurements, however, tend to bias the true values. Hence, before the data can be analyzed, they should be carefully quality controlled, calibrated, and validated. A number of efforts have been conducted for this purpose. More recently, three consistent, long-term, and multiplatform altimeter datasets have been established and continuously updated—the global altimeter significant wave height (SWH) dataset (Queffeulou 2004 and Queffeulou and Croizé-Fillon 2016), the Global Wave Project (Ash 2010), and the joint calibrated multiplatform altimeter data (Zieger et al. 2009)—with the first two relating to each other (Queffeulou 2013b). The work presented in this paper is the initial attempt to incorporate the *HY-2* altimeter data into the third dataset.

There have been several published works assessing *HY-2* H_s measurements; these have consistently demonstrated its good quality (Yang et al. 2014; Chen et al. 2013; Wang et al. 2013; Zhang et al. 2015; Ye et al. 2015). The first three works focused on the preliminary calibration of *HY-2* wave observations shortly after its launch, while the latter two considered a rather long duration of measurements (>2 yr). A conclusion, however, can be drawn that *HY-2* tends to overestimate low H_s (<1 m) and underestimate wave heights throughout the remaining range of heights, especially for high seas, $H_s > 5$ m (e.g., Chen et al. 2013; Zhang et al. 2015). The overall negative bias is ~0.2 m and the root-mean-square error (RMSE) is ~0.3 m (see also Table 2). However, regardless of this nonlinear bias, all of these studies employed a linear regression method for calibration. Though significantly decreasing the overall RMSE, such linear correction could not remove the apparent mismatch between *HY-2* and other satellite missions, like *Jason-2* for high seas (e.g., see Fig. 5 of Zhang et al. (2015); our Fig. 3). This deficiency would severely constrain the application of the *HY-2* altimeter data in monitoring high seas, for example, in tropical cyclones. Motivated by this, we reanalyzed the available *HY-2* wave products against in situ buoys and other satellite altimeters with the objective of refining its existing calibration. Another motivation was the result reported by Ye et al. (2015) that the accuracy of *HY-2* H_s measurements varies with time. Based on measurement performance, they subdivided the whole data period studied into three phases. They, however, did not provide a separate calibration for each phase; thus leaving such an effort for further improvement to this study.

Compared to the extensive attention paid to H_s, efforts made to investigate *HY-2* altimeter-measured U_{10} are rare. To the authors' knowledge, the only published work on altimeter-measured U_{10} was conducted by Jia et al. (2014). These authors used only less than 1 month of data for a very preliminary assessment. By employing the two-parameter wind model proposed in Gourrion et al. (2002), they reported that the RMSE of their wind speed determinations was within 2 m s^{-1}, satisfying the required accuracy of the *HY-2* mission. Given this, we also carried out a thorough analysis of *HY-2* U_{10} measurements in order to fill in the gap of studies of this sort. Adopting the wind model described in Abdalla (2012), we were able to further improve the accuracy. Our results, however, are not described in this article. This is because the NSOAS agency is reprocessing *HY-2* altimeter data by using a different retracking algorithm. The forthcoming new data are expected to have better quality U_{10} measurements and sea surface height h but only a limited improvement in H_s measurements (see also section 5 of Zhang et al. 2015). Therefore, wind products from the *HY-2* altimeter measurements are left for future reassessment.

This article is organized as follows. Section 2 presents the data and methods we used to evaluate *HY-2* H_s measurements. Section 3 shows the overall calibration of *HY-2* H_s data against buoys and the cross validation against other concurrently operated satellite altimeters. Section 4 proposes our revised calibration for *HY-2* H_s measurements, followed by a further discussion in section 5, in which we use data produced by a wave model to demonstrate the validity of our calibration. A brief conclusion in section 6 finalizes this paper.

2. Data and methods

a. Quality control

We analyzed geophysical records from four satellite altimeters: *HY-2*, *CryoSat-2*, *Jason-2*, and *SARAL*. Data from *HY-2* and *CryoSat-2* are denoted as the interim geophysical data records (IGDRs), while data for the other two missions are referred to as the geophysical data records (GDRs). Table 1 summarizes the information regarding these data, including their sources, data periods, and the orbit parameters of each mission. Except for *SARAL*, all the missions have provided records for more than 3 yr.

As far as the calibration of altimeter products is concerned, the first step is to quality control them—that is, to remove the erroneous or suspicious records normally through using a number of empirical criteria. These criteria should not be so rigorous or loose that the calibration and statistics we finally obtain are unrepresentative (Cotton et al. 2003). Basically, the methods of quality control can be roughly categorized into two groups. Both groups rely on the basic flags for altimeter records; for example, land, ice, rain flags, other 1-Hz quality flags, and the number of valid waveforms that make up the 1-Hz sample. The first group, furthermore, depends on additional auxiliary information, such as range R, off-nadir angle, peakiness, and the standard deviation (std) of H_s measurements. One should make sure these parameters fall into reasonable ranges that usually can be obtained from handbooks and statistical analyses (e.g., see the appendix of Mackay et al. 2008; Ash 2010). Noteworthy, based on the fact that the logarithm of the std of H_s can be approximately considered to be Gaussian distributed (e.g., Queffeulou 2004), an upper limit of the std of H_s is usually set up to identify ‘‘bad’’ records. This characteristic is shared by many missions, such as *Jason-1*, the *Environmental Satellite* (*Envisat*; Queffeulou 2004), and *SARAL* (Sepùlveda et al. 2015), and also holds true for *HY-2*. The methods from the first group, however, are somewhat laborious because the thresholds–criteria are normally platform dependent. Thus, we should analyze each mission separately to find reasonable criteria (e.g., Cotton et al. 2003).

The second group uses a more straightforward and also a very efficient method. Under the assumption that the sea state will not change dramatically within a limited geophysical scale say less than ~200 km, altimeter records along the track are divided into blocks of ~25 observations for a further statistical consistency check (Young and Holland 1996; Zieger et al. 2009; Queffeulou and Croizé-Fillon 2016). Spikes or outliers within each block—that is, values that deviate significantly from the mean value of the block—are flagged as bad. Not only intuitive, methods of this kind can also be directly applied to various missions with a slight modification of block size that depends only on the ground scanning speed of each satellite altimeter. A combination of these two groups is also feasible (Abdalla and Hersbach 2004). Following Young and Holland (1996), we chose the second method for the purpose of quality control. For further details of this three-pass procedure, please also refer to Zieger (2010). The proportion of the ‘‘flagged’’ records for the four altimeters used in our work is also shown in Table 1 (last column). Note that *HY-2* has the highest percentage (21%).

b. Calibration against in situ measurements

Although not free of errors, the in situ measurements are always regarded as ground truth and were applied to calibrate satellite measurements and to validate wave models (e.g., Bidlot et al. 2002; Li and Saulter 2014). Of all globally operating buoy networks, data from the buoys maintained by the U.S. National Data Buoy Center (NDBC) are most widely used and referenced in the literature due to their excellent quality and long duration, dating back to the early 1970s. After being quality controlled by NDBC staff, the historical NDBC data are archived at the National Oceanographic Data Center (NODC). For this paper, we obtained data for the period from 1 October 2011 to 31 November 2014, which nearly covers the durations of all available altimeter records. Only buoys located more than 40 km offshore were considered in order to avoid the heavily seaward sampling problem when a buoy is too close to a coastline (Greenslade and Young 2004). This criterion finally yielded 63 stations, whose locations are shown in Fig. 1. Although the buoy data were checked by a number of quality-control procedures, a few erroneous values are still unflagged (not shown). Therefore, an additional quality control was carried out in a fashion similar to the method described in Caires and Sterl (2003). More precisely, wave measurements that (i) are too extreme—that is, $H_s < 0.15$ m or $H_s > 30$ m—and (ii) deviate more than 6 times the std of the monthly data from the monthly mean or more than 2 times the std of the monthly data from previous measurements are discarded.

Using the criteria of 50 km for spatial separation and 30 min for time difference (Monaldo 1988), we calculated

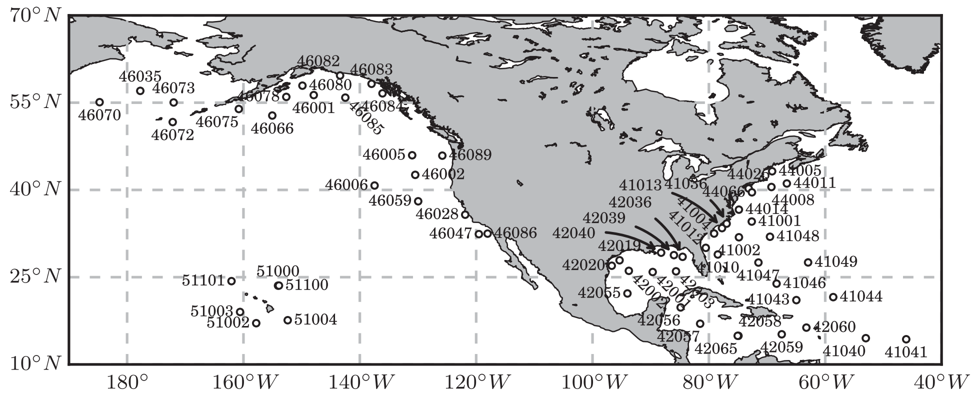

Fig. 1. The locations of the 63 NDBC buoys (empty circles) used in the study. Only buoys more than 40 km offshore are listed and some buoys could have drifted somewhat or been redeployed during the period of study.

the average values along satellite altimeter transects (~15 observations) and linearly interpolated the value to the nearest hourly or half-hourly buoy records (e.g., Queffeulou 2004; Zieger et al. 2009; Durrant et al. 2009). Only transects with more than four valid 1-Hz records were used. Once all the possible altimeter–buoy collocations were located, the reduced major axis (RMA) regression procedure was used to calibrate the altimeter data, with major outliers being eliminated by robust regression (Zieger et al. 2009). Note that other techniques like orthogonal regression and ordinary least squares can also be used to establish the best fit between a buoy and an altimeter measurement (e.g., Queffeulou 2004; Durrant et al. 2009; Ray and Beckley 2012). Other calibration techniques, such as two-branch linear functions or high-order polynomials, were also investigated. The four following statistical parameters: bias b, RMSE ε, correlation coefficient ρ, and the scatter index SI, were utilized to evaluate the performance of the altimeter estimates:

$$b = \frac{1}{N}\sum_{i=1}^{N}(x_i - y_i), \tag{1}$$

$$\varepsilon = \sqrt{\frac{1}{N}\sum_{i=1}^{N}(x_i - y_i)^2}, \tag{2}$$

$$\rho = \frac{\sum_{i=1}^{N}(x_i - \overline{x})(y_i - \overline{y})}{\sqrt{\sum_{i=1}^{N}(x_i - \overline{x})^2 \sum_{i=1}^{N}(y_i - \overline{y})^2}}, \tag{3}$$

$$\mathrm{SI} = \frac{\sqrt{\frac{1}{N}\sum_{i=1}^{N}[(x_i - \overline{x}) - (y_i - \overline{y})]^2}}{\overline{y}}, \tag{4}$$

where x and y represent the estimates from two different platforms, for example, buoy, altimeter, or model; the bar over x and y denotes their mean value; and N is the number of collocated measurements. When necessary ε^*, which signifies the RMSE between the calibrated altimeter values and estimates from other platforms, together with the number of outliers N_{out} among the collocated data, were also used to illustrate the effect of our calibrations.

c. *Cross validation against other altimeters*

The altimeter–buoy collocated data were basically limited to an area off the U.S. coastline; therefore, altimeter measurements needed to be further validated against other simultaneously operating altimeters on a global scale. For *HY-2* validations, three other missions were available: *Jason-2*, *CryoSat-2*, and *SARAL*. *Jason-2* and *CryoSat-2* operate on the same Ku-band frequency as *HY-2*. *SARAL* operates in the high-frequency Ka band (35.75 GHz), which reduces the size of the altimetry footprint and provides better spatial and vertical resolutions. This Ka band–operated altimeter is expected to provide more accurate H_s and an improved performance along coast lines (Hithin et al. 2015, see also our section 3). These advantages are, however, countered by the fact that Ka band is more sensitive to water vapor and cloud cover than Ku band, and therefore the transfer function needed to derive wind speed would need to be revisited (e.g., Lillibridge et al. 2014).

To confidently use H_s measurements from these three altimeters, we first needed to calibrate them against buoys in the same way as previously mentioned and then undertake a cross-validating procedure by analyzing the altimeter to altimeter collocated data, that is, dual-satellite crossovers (Kim 1997) within a 30-min separation. A 100-km along-track average (50 km at each side

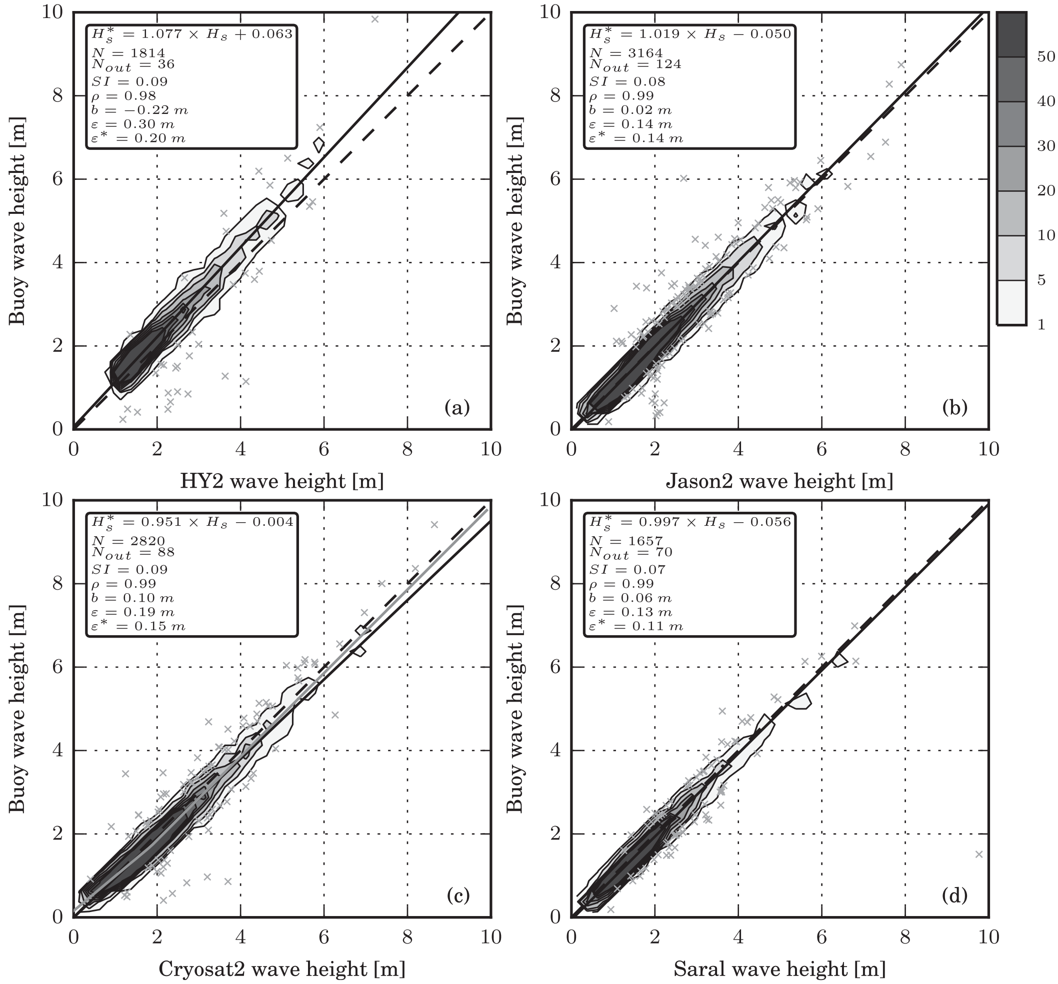

FIG. 2. The calibration results for the H_s measurements from the four altimeters used in the study vs the collocated buoy measurements. (a)–(d) The altimeters on satellites: *HY-2*, *Jason-2*, *CryoSat-2*, and *SARAL*, respectively. The number of collocated measurements in each $0.25 \times 0.25\,\mathrm{m}^2$ bin is color shaded and contoured, and the × symbols represent the outliers identified by robust regression. The black dashed line is the 1:1 line and the solid line denotes the calibration estimated by RMA regression. Its formula and statistical parameters: b, ε, ρ, and SI, defined by Eqs. (1)–(4), together with N and N_{out} are given in the inset. The ε^* signifies the RMSE after RMA calibration. The solid gray line in (c) is the two-branch linear calibration for *CryoSat-2* H_s measurements given by Eq. (6).

of crossovers) of altimeter transects, containing at least 10 valid 1-Hz records, was finally used. Altimeter–altimeter collocated measurements were processed in the same way as was done for the altimeter–buoy collocated measurements (section 2b). In order to detect any variation (jump or drift) of altimeter performance, time series of the differences between altimeter pairs were also investigated (Zieger et al. 2009).

d. Further verification against wave model

Although the period of the altimeter data we considered was relatively long (e.g., >3 yr for *HY-2*), the altimeter–buoy and altimeter–altimeter collocated measurements were still limited in total number, usually of the order of $O(10^3)$ (section 3). In addition, high sea states ($H_s > 6\,\mathrm{m}$) were less frequently sampled by these collocated measurements (Fig. 2). Because we wanted to increase the number of collocated points for the calibration of *HY-2* H_s measurements, in particular for high seas, we looked at matchups between *HY-2* estimates and modeled significant wave height. With the extensive efforts of the wave modeling community over the past several decades and the increasing quality of the wind-driven forcing (e.g., wind fields), wave models nowadays are capable of providing a satisfactory estimate of the sea state, particularly of H_s. A very thorough review of this wide topic is given in Cavaleri et al. (2007). Moreover, most recently, the National Oceanographic Partnership

Program (NOPP; Tolman et al. 2013) dedicated to transition the latest advances in wave science to operational wave models has made several new source term packages available (e.g., Ardhuin et al. 2010; Filipot and Ardhuin 2012; Donelan et al. 2006; Babanin et al. 2010; Rogers et al. 2012; Zieger et al. 2015) and the performance of wave models has been further enhanced.

Modeled wave heights were sourced from the Integrated Ocean Waves for Geophysical and Other Application (IOWAGA) database [Institut Fançais de Recherche pour l'Exploitation de la Mer (Ifremer); http://wwz.ifremer.fr/iowaga], which is available at a resolution of 0.5° spatially and 3-hourly temporally. The database is based on WAVEWATCH III using the semiempirical parameterizations (ST4, TEST471). The reader is referred to Ardhuin et al. (2010), Filipot and Ardhuin (2012), Rascle and Ardhuin (2013), and Leckler et al. (2013) for details. Instead of calibrating the satellite data again, the main objective was to demonstrate the validity of our calibration. Thus, we used only 2 months of data (January 2013 and January 2014) for a very simple illustration. As mentioned in Rascle and Ardhuin (2013), when driven by ECMWF operational winds, the Ifremer wave model presents an obvious negative bias in H_s predictions for very high seas as a result of the bias existing in the ECMWF winds (see their Figs. 1 and 2). A simple linear correction is proposed by Ifremer for the years 2006–11, given by

$$H_s^* = \begin{cases} H_s & H_s \le 8\,\text{m} \\ 1.25 \times (H_s - 8) + 8 & H_s > 8\,\text{m} \end{cases}, \qquad (5)$$

where H_s and H_s^* are the raw and corrected wave heights, respectively. We assumed this correction was still applicable for 2013 and 2014, which proved to be reasonable in section 5. The altimeter-measured H_s was collocated with model products in a similar way as in Rascle et al. (2008). First, the modeled H_s was interpolated bilinearly in space and linearly in time to the altimeter-measured H_s. And then these interpolated values, together with their 1-Hz altimeter counterparts, were averaged along the track into 1° bins.

3. Results

a. Calibration against buoys

An overall comparison of H_s measurements between the four altimeters and buoy-measurements is presented in Fig. 2. In general, agreements between all the four altimeters and the buoys are very good with high correlation (≥0.98), low RMSE (≤0.30 m), and a small scatter index (≤0.09).

1) *HY-2*

Performance of the *HY-2* H_s measurements is illustrated in Fig. 2a. Based on 1814 collocations, *HY-2* has a slightly high negative bias (−0.22 m), a very high correlation coefficient (0.98), and a low RMSE (0.3 m) that is within the stated accuracy (0.5 m). These statistics agree well with the existing studies on *HY-2* H_s measurements as summarized in Table 2. The slope and intercept of the RMA regression are 1.077 and 0.063, respectively, comparable with those of Chen et al. (2013). Seen in Fig. 2a, an underestimation tendency of *HY-2* H_s measurements exists throughout the whole range (1–6 m) and becomes a little more marked for higher values. This is consistent with other studies (e.g., Zhang et al. 2015). The overestimation tendency for low sea states ($H_s < 1$ m) as addressed in previous studies is, however, absent here due to a severe dearth of small values in our quality-controlled dataset. This lack of small wave height data may have two implications. First, the method we used for quality control (section 2a) may be somewhat too strict for *HY-2*, although it has been used for previous satellite altimeters (Zieger et al. 2009; Zieger 2010). Second, wave height estimates of less than 1 m tend to be suspicious or erroneous as previously reported by Zhang et al. (2015, see their Figs. 3 and 4). They indicated that at low sea states, *HY-2* measurements are either invalid or severely overestimated, and they speculated that this strange behavior might be associated with the limitation of the data retrieval algorithm. The hooklike data cluster for *HY-2* and *Jason-2* collocated measurements shown in the lower-left corner of their Fig. 5a also shows the strong gradient of *HY-2* wave height estimates within this narrow range. Therefore, the absence of low values in our data is probably not caused by our quality-control procedure. Another peculiarity of *HY-2* is that the total number of its collocations with buoy measurements is far below those for *Jason-2* and *CryoSat-2* (Figs. 2b and 2c), although they span the same duration. As explained in Zhang et al. (2015), this is mainly caused by the high proportion of missing–invalid records in *HY-2* IGDRs (see also Raynal 2014). The RMA regression reduces the RMSE to 0.2 m, which is a considerable 33%. However, as we can see in the section 3b, this needs to be further reduced.

2) Other three altimeters

There are many studies that address the quality of wave height measurements as estimated by the *Jason-2*, *CryoSat-2*, and *SARAL* altimeters (e.g., Queffeulou et al. 2011; Ray and Beckley 2012; Sepùlveda et al. 2015; Zhang et al. 2015). The differences in the calibration results from these studies are usually caused by inconsistent methods of data processing. Therefore, we applied the same calibration procedure to these three altimeters for consistency and show their performances in Figs. 2b–d.

A total of 3164 collocations between *Jason-2* and buoys (Fig. 2b) show a significant correlation (0.99), an RMSE as low as 0.14 m, and a negligible bias (0.02 m). The RMA regression is very close to the 1:1 line. All the metrics demonstrate the high quality of *Jason-2* H_s measurements, agreeing well with other studies. It is worth mentioning that both Queffeulou et al. (2011) and Ray and Beckley (2012) found a negative bias of a few centimeters, while Sepùlveda et al. (2015) and Zhang et al. (2015) showed a positive bias, which is similar to our results. Since both the latter two studies and our work focus on the most recent *Jason-2* data this might indicate that *Jason-2* wave products may have had a marginal change in the past several years. Another factor possibly responsible for this slight difference might be the different version of *Jason-2* GDRs [GDR, version T (GDR-T); or GDR, version D (GDR-D)] used by these authors.

For *CryoSat-2*, data from 2820 collocations are presented in Fig. 2c; these display a slightly higher bias (0.10 m) and RMSE (0.19 m) compared to those from *Jason-2* measurements. Compared to *Jason-2*, *CryoSat-2* measurements show a nonlinear bias. *CryoSat-2* tends to underestimate H_s for low values ($H_s < 1$ m) and overestimate high values. Queffeulou (2013a) found the same feature and proposed a two-branched function to correct *CryoSat-2* H_s measurements (see their Figs. 7 and 8) that consists of a third-order polynomial for low values and a linear adjustment for high values. We, following Greenslade and Young (2004), use a rather simple two-branched linear correction to eliminate this nonlinear bias, given by

$$H_s^* = \begin{cases} 0.836 \times H_s + 0.157 & H_s \le 1.853\,\text{m} \\ 1.001 \times H_s - 0.149 & H_s > 1.853\,\text{m} \end{cases}. \qquad (6)$$

This two-branched correction, shown as a gray line in Fig. 2c, reduces the RMSE from 0.19 to 0.14 m and thereby improves the accuracy of *CryoSat-2* H_s measurements to the same level as those from *Jason-2*.

Among the four altimeters considered in this article, measurements from the *SARAL* mission are of the highest quality. In Fig. 2d, *SARAL* measurements show the lowest RMSE (0.13 m) and scatter index (0.07). But they have a slightly higher bias (0.06 m) than that of *Jason-2* measurements. Also, the RMA regression can further decrease the RMSE to 0.11 m. Sepùlveda et al. (2015) also pointed out that *SARAL* measurements has a slightly larger bias but lower RMSE than *Jason-2* measurements. Since, as mentioned in section 2b, *SARAL* is capable of providing a high spatial and vertical resolution, it is not surprising that *SARAL* is superior to the Ku-band altimeters. Most importantly, its performance along coastlines is also fairly encouraging. Hithin et al. (2015) analyzed *SARAL* H_s measurements in coastal ocean and inland waters, and concluded that *SARAL* gave a very good performance near the coast (6-cm bias and 19-cm RMSE). In the coastal zone (<2 km from coast), *SARAL* measurements have a high correlation (0.94) and a low RMSE (0.24 m), with which even the *Jason-2* products optimized for coastal application cannot compete.

To summarize briefly, among the four altimeters, *SARAL* H_s measurements are the best in performance, followed by wave height measurements from *Jason-2*, *CryoSat-2*, and *HY-2*. Nonetheless, the *HY-2* H_s measurements are still well within the NSOAS required accuracies and are highly correlated with buoy observations.

b. Cross validation against other altimeters

For *HY-2* H_s measurements, the deficiency in the RMA regression shown in Fig. 2a or any other corrections described in previous studies (see Table 2) are clearly shown in this subsection. The collocation data for the four altimeters are shown in Fig. 3, and the time variations of the differences between specific pairs of altimeters are presented in Fig. 4. Note that all the wave heights presented in these two figures were already corrected by the calibration procedures presented in section 3a.

Inspection of Fig. 3 shows that the agreement between *Jason-2*-, *CryoSat-2*-, and *SARAL*-calibrated H_s measurements is very good (Figs. 3d–f). An almost perfect agreement can be found in *SARAL*–*Jason-2* collocated measurements (Fig. 3d) with a correlation coefficient of 1 and a 0 bias. Since all satellite altimeters use the same principles to sense the ocean surface, the altimeter–altimeter collocated measurements are less scattered than those between altimeter and buoy measurements. For example, for *SARAL*, the RMSE relative to *Jason-2* is 0.07 m, compared to 0.11 m relative to buoys [see also Zieger et al. (2009) for previous missions]. The excellent consistency between the three different satellite measurements reveals that (i) the calibration proposed in section 3a for each satellite is reasonable, especially the two-branch correction for *CryoSat-2* [Eq. (6)], which effectively eliminates its nonlinear bias; and (ii) although all the calibrations are derived from a range of wave heights of 0–6 m, the calibrations also perform well for high sea states (6 m $< H_s <$ 10 m). These conclusions, however, do not hold for *HY-2* measurements. An

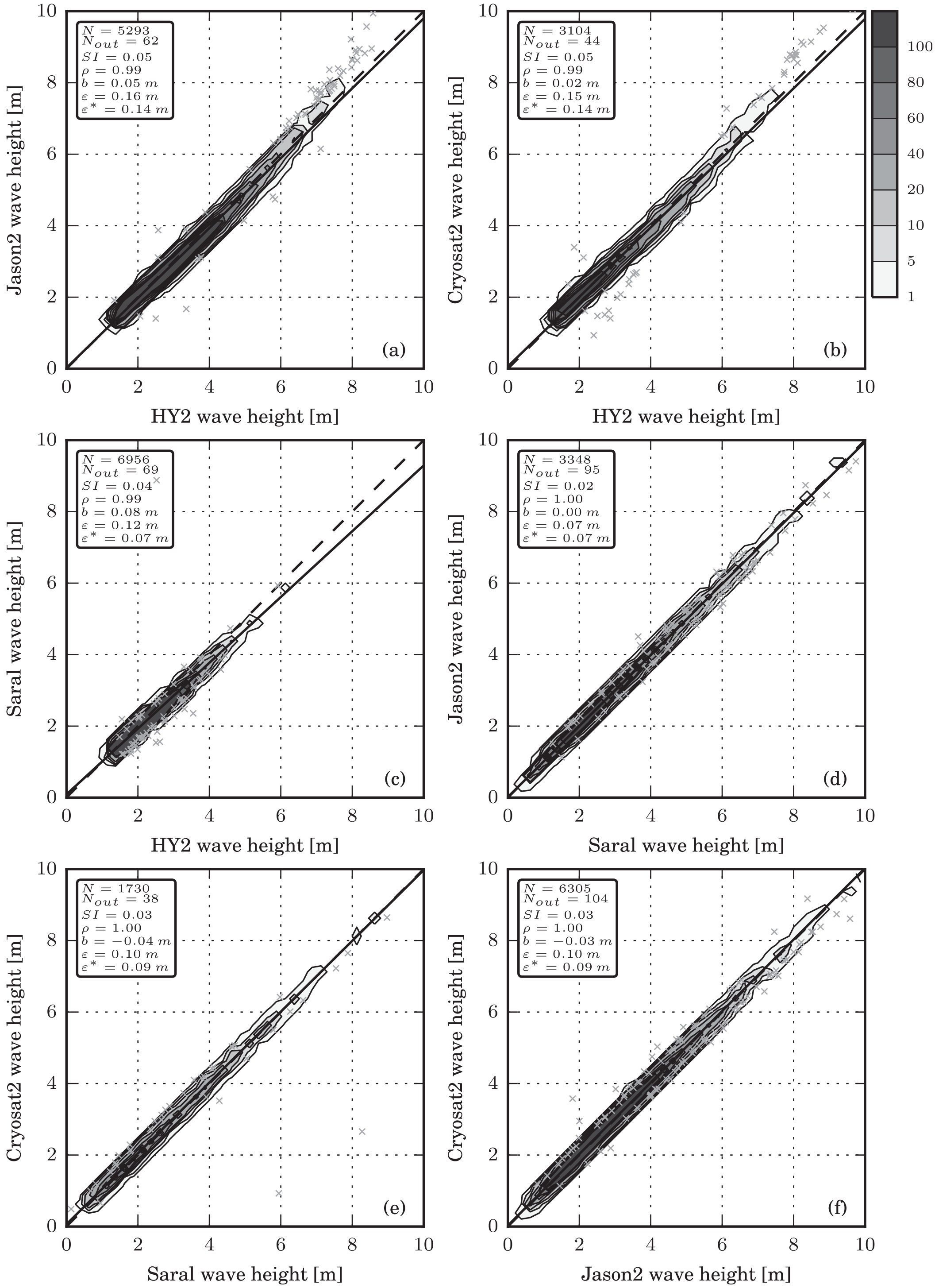

FIG. 3. The cross-validation results for calibrated H_s measurements (see section 3a) from the different altimeters: (a)–(f) *HY-2–Jason-2*, *HY-2–CryoSat-2*, *HY-2–SARAL*, *SARAL–Jason-2*, *SARAL–CryoSat-2*, and Jason2–*CryoSat-2*, respectively. Shaded contours and statistical parameters are as in Fig. 2, except that the RMA regression formulas are not shown.

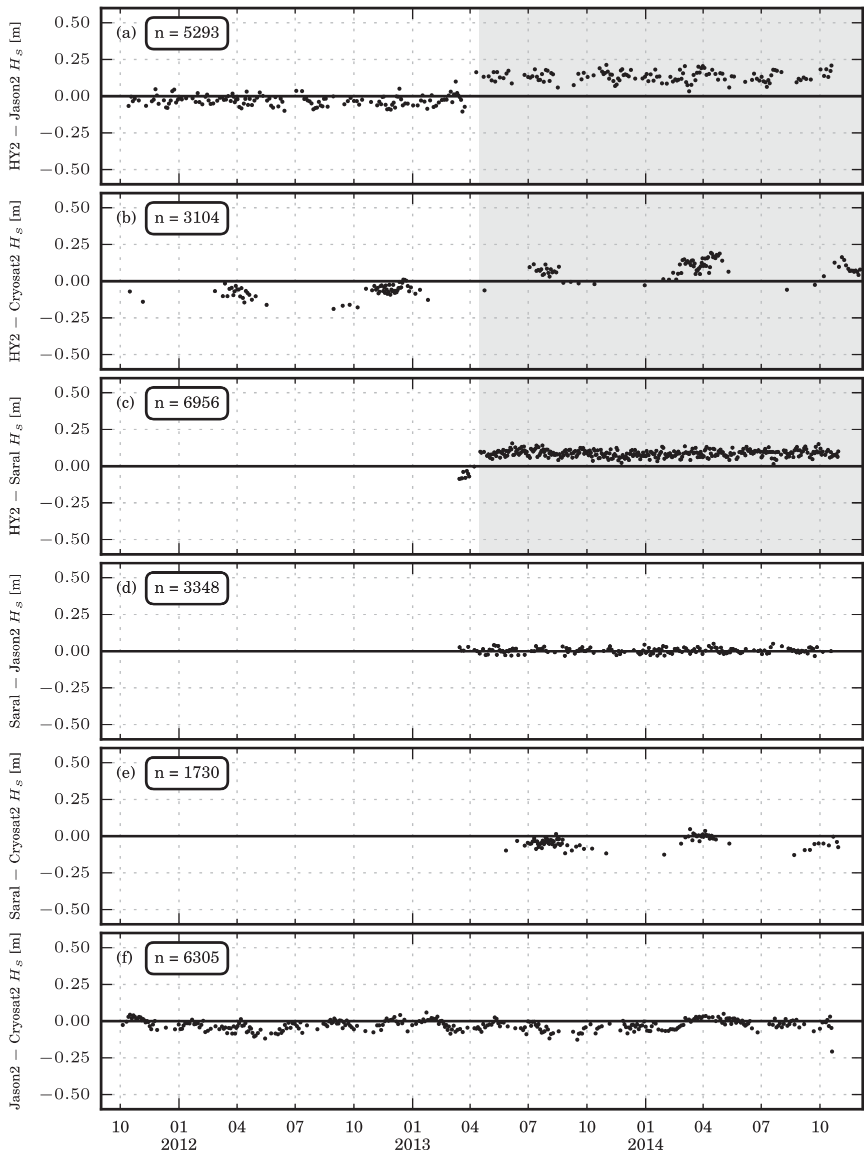

FIG. 4. The October 2011–2014 time series of the differences between calibrated H_s measurements (see section 3a) from (top to bottom) the altimeter pairs in Fig. 3 (20 block averages). (a)–(c) The shaded areas denote a time discontinuity in *HY-2* H_s measurement performance. The black horizontal solid line in each panel highlights the zero line.

examination of Figs. 3a–c shows that although calibrated *HY-2*-H_s measurements agree well with the measurements from the other three satellites, several incompatibilities can be found. First, *HY-2* measurements present a positive bias relative to the other three altimeters; that is, after being calibrated by the RMA regression, *HY-2* H_s measurements are inclined to overestimate the sea state. This is most evident when compared with *SARAL* (Fig. 3c). Second, when $H_s > 6$ m, an apparent mismatch between *HY-2* and *Jason-2*/*CryoSat-2* measurements exists (Figs. 3a and 3b); this is represented by the upward bend of the shaded contours and the appearance of the small cluster of outliers. This mismatch is absent in collocation measurements between *HY-2* and *SARAL* because their crossovers are constrained to low latitudes (30°S–30°N). As previously described, these other three altimeters have a very consistent behavior; therefore, we conclude that the RMA regression procedure for *HY-2* should be further revised.

Another shortcoming of the *HY-2* RMA calibration is displayed in Fig. 4, where the difference between altimeter–altimeter collocated measurements is shown as a function of time. For better visualization, block averages over 20 points have been used (Zieger et al. 2009). Similar to what has been seen above, differences between *Jason-2*, *CryoSat-2*, and *SARAL* (Figs. 4d–f) are relatively insignificant and remain so with time. Only a bias of a few centimeters is to be expected between *CryoSat-2* and *Jason-2*/*SARAL* (see also Figs. 3e and 3f). A noticeable jump in *HY-2*-measured H_s values occurred in April 2013 and is consistently captured in Figs. 4a–c (the shaded area). According to NSOAS, this jump is related to the switch of *HY-2* to backup status and the subsequent update of data processing software. On the basis of monthly bias and the RMSE of *HY-2* H_s relative to NDBC buoys, Ye et al. (2015) subdivided their data period into three phases: the first phase for the period from October 2011 to September 2012, the second for the duration from October 2012 to March 2013, and the third for the period after April 2013. They reported that the RMSE of *HY-2* H_s measurements was around 0.4 m during the first phase, increased to ~0.5 m in the second phase, and then improved to 0.3 m after April 2013 in the third phase. The decline of *HY-2* H_s measurement accuracy in their second phase, however, is not obvious in our Fig. 4 (see also Fig. 7), which might be ascribed to the differences between our data processing methods. Nevertheless, the *HY-2* σ_0 of this period indeed became more scattered (not shown), indicating that electronic drift and sensor degradations could have taken place. Since we only address wave measurements in this article, which are unrelated to the backscatter σ_0, we chose to divide the data period of *HY-2* H_s measurements shown in Fig. 4 into two phases: phase 1 for the period from 1 October 2011 to 1 April 2013 (cycle < 41) and phase 2 for the period from 15 April 2013 and after (cycle ≥ 41).[1]

4. Revised calibration of *HY-2* H_s measurements

As explained in the previous section, *HY-2* H_s data behaved differently in the two separate phases and presented a significant underestimation for high sea states, making the linear RMA best fit formulated in Fig. 2a impractical. In this section, a revised two-branch calibration method for *HY-2* H_s measurements is proposed for both phase 1 and phase 2.

The best way to calibrate altimeter wave height is undoubtedly to use in situ buoy measurements as we did in section 3a. Nonetheless, for *HY-2* measurements, there were only very few buoy collocations when sampling high seas (Fig. 2a) and thus this presented difficulties for our study. Considering the excellent consistency between *Jason-2*-, *CryoSat-2*-, and *SARAL*-calibrated H_s measurements (Figs. 3 and 4) throughout the 0–10-m range, we resorted to adopting measurements from these three satellites for this recalibration objective. This method is appropriate and has been employed by Queffeulou (2013a) to calibrate *CryoSat-2* H_s measurements in a global sense.

In Fig. 3, the negative bias in *HY-2* H_s measurements present at high H_s values is clearly illustrated by its *Jason-2* and *CryoSat-2* collocated measurements (Figs. 3a and 3b). We opted to regard the corrected *Jason-2* H_s measurements as reference, leaving *CryoSat-2* values as a uniquely independent source to verify the revised calibration, especially for high sea conditions. Following Queffeulou (2013a), the collocated *HY-2* and *Jason-2* measurements shown in Fig. 3a were grouped into 0.25-m bins and averages and stds were calculated and are shown in Fig. 5. Afterward from these binned statistics, a two-branch correction was fitted that consists of a linear function for small waves and a second-order polynomial for large waves as given by Eq. (7) and (8) for phase 1 and phase 2, respectively,

phase 1 (cycle < 41):

$$H_s^* = \begin{cases} 1.003 \times H_s + 0.287 & H_s \leq 3.504\,\text{m} \\ 0.040 \times H_s^2 + 0.838 \times H_s + 0.376 & H_s > 3.504\,\text{m} \end{cases}, \tag{7}$$

phase 2 (cycle ≥ 41):

$$H_s^* = \begin{cases} 0.977 \times H_s + 0.187 & H_s \leq 3.568\,\text{m} \\ 0.013 \times H_s^2 + 1.083 \times H_s - 0.359 & H_s > 3.568\,\text{m} \end{cases}. \tag{8}$$

Once again, an examination of Fig. 5 shows that the negative and nonlinear bias in *HY-2* H_s measurements is present in each phase. The two-branched corrections (black solid lines) are capable of following the upward bends of shaded contours that are present in the 5–7-m wave height range. Moreover, the two-branched calibration in Fig. 5b is closer to unity than that in Fig. 5a, which in fact demonstrates the better quality of *HY-2* wave products in the second phase. We note that for phase 1, the nonlinear bias of *HY-2* H_s measurements relative to *Jason-2* previously had been fitted by Chen et al. (2013) with a fifth-order polynomial; however, they finally applied a linear regression method to calibrate *HY-2* wave estimates.

The *HY*-2 measured-wave heights calibrated using Eqs. (7) and (8), were again compared to collocated-buoy

[1] There were no *HY-2* data from 2 to 13 April 2013 due to the instrument maintenance.

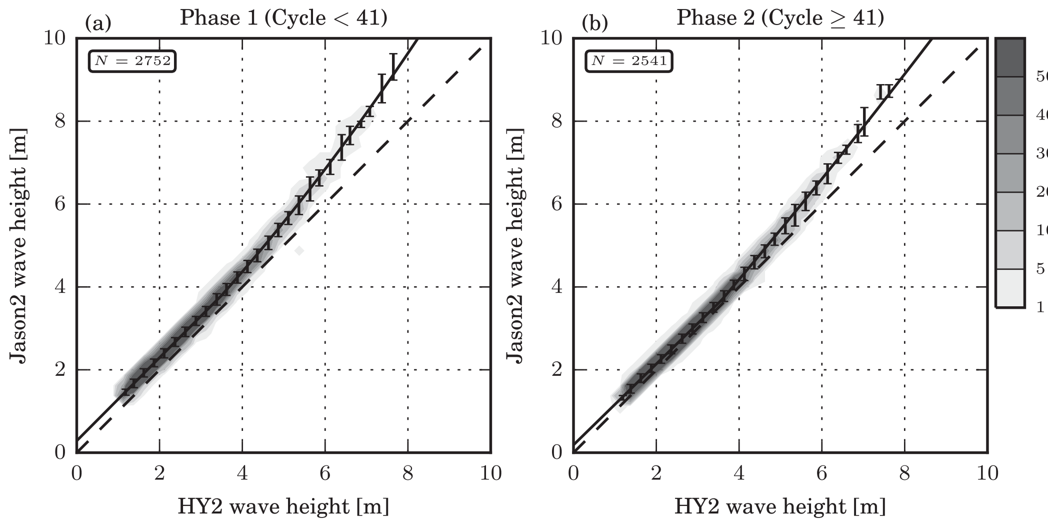

FIG. 5. The revised two-branch calibration of the *HY-2* H_s measurements: (a) phase 1 and (b) phase 2. The x axis represents the raw *HY-2* H_s values, while the y axis represents the calibrated *Jason-2* H_s values (Fig. 2). The black solid curve in each panel denotes the two-branch calibrations given by Eqs. (7) and (8) and the error bars on either side of the average values represent the stds in every 0.25-m bin. Other elements in this figure are as in Fig. 2.

measurements and the values from the other three satellite altimeters (calibrated values) in Fig. 6. When compared to buoys (Fig. 6a), *HY-2* wave height estimates now are almost unbiased (0.01 m) and have a much lower RMSE of 0.17 m versus 0.30 m for the uncorrected data (Fig. 2a). The RMA best fit is nearly equal to 1, proving that using *Jason-2*-calibrated H_s measurements as the ground truth, does not trigger any incompatibility with in situ observations. Since Eqs. (7) and (8) are derived from *Jason-2*-corrected H_s values, it is not surprising that after the calibration, *HY-2* and *Jason-2* are in excellent agreement (Fig. 6b), represented by the zero bias and full linear correlation.[2] The most encouraging result is displayed in Fig. 6c, where *HY-2* and *CryoSat-2* collocated data are illustrated. Here, the mismatch between *HY-2* and *CryoSat-2* shown in Fig. 3b is absent. The RMSE also decreased from 0.15 to 0.11 m. Improvements can also be seen in the collocated data differences between *HY-2* and *SARAL*. In Fig. 3c, *HY-2* is clearly overestimating sea states in the 3–5 m range; while in Fig. 6d, these two altimeters on different platforms agree much better, as indicated by the decrease of RMSE from 0.12 to 0.07 m. To check whether the revised calibration eliminates the time discontinuity displayed in Figs. 4a–c, the variation with time of the difference between *HY-2* and buoy measurements is plotted in Fig. 7. Statistics for *HY-2* measurements relative to the buoys can also be seen in Table 3. For phase 1 (the third row of Table 3) *HY-2* raw wave data show a bias of −0.31 m and an RMSE of 0.37 m; while for phase 2 (the fourth row in Table 3) the bias and RMSE are considerably improved to −0.13 and 0.21 m, respectively, approaching the quality level of *CryoSat-2*. Our final calibration turned out to be effective, especially for phase 1 in which the RMSE decreased from 0.37 to 0.19 m. Furthermore, the marginal distinction between RMSEs of *HY-2*-calibrated H_s values from the two phases (0.19 and 0.16 m, respectively) indicates that the quality of each phase is now similar. Visually, the sign of this improvement can be seen in Fig. 7, where the bias between *HY-2*-calibrated H_s and buoy measurements are clustered around the horizontal zero line without any conspicuous jump.

[2] When more data are available in the future, a method that uses half of the reference data for calibration and the other half for validation is preferred.

5. Discussion

This section focuses on verifying the practical applicability of our revised calibration provided in the section above. One may argue that the dataset we used to fit the calibrations Eqs. (7) and (8) is limited and less representative for real high seas. Here, we attempt to indirectly prove the validity of the revised calibration. Numerical wave models can provide excellent resolution in both temporal and spatial scales. Comparing altimeter data to a model can definitely increase the sample size of the collocated dataset and, consequently, the probability of representing a wide variety of sea states. However, since wave models are inclined to be

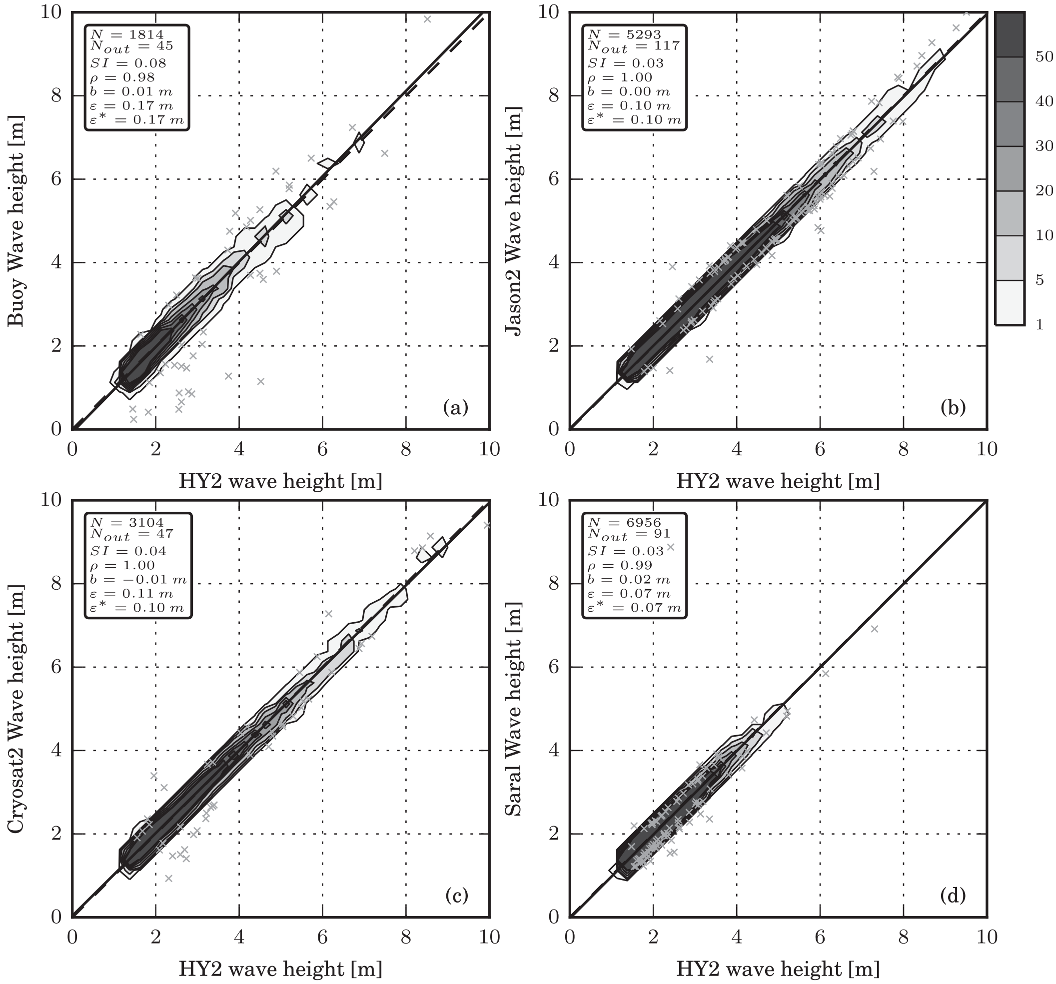

FIG. 6. As in Fig. 3, but for *HY-2* H_s measurements calibrated by Eqs. (7) and (8). Collocated measurements from (a) *HY-2* and the buoys and (b)–(d) the other three altimeters (calibrated value; see section 3a).

less accurate than altimeters, we avoid using them for the ground truth. Instead, we compared both *HY-2*- and *Jason-2*-calibrated H_s values to wave model estimates. If the two altimeters yield similar patterns and statistics, then we could conclude that if adopting our calibration, results in *HY-2* H_s values are to some degree similar to *Jason-2* ones—then these calibrated *HY-2* H_s values are now more realistic.

Since we just wanted to demonstrate the validity of our calibration, we used only two-months of model data, consisting of January 2013 from phase 1 and January 2014 from phase 2 of *HY-2* measurements. The comparison between *Jason-2–HY-2* and the wave model is shown in Fig. 8. For both *Jason-2* and *HY-2*, more than 50 000 instances of collocated measuremnts were obtained for each month. Focusing first on *Jason-2* (Figs. 8a and 8d), the agreement between *Jason*-2 results and the wave model is quite good: for each month, the correlation coefficient is 0.97 and the scatter index is 0.12. The comparison of January 2013 shows a bias of 0.11 m and an RMSE of 0.34 m; while January 2014 gives slightly improved result (a bias of 0.07 m and an RMSE of 0.31 m). These statistics are very similar to the results of Zieger et al. (2015, see the middle panel of their Fig. 13). The difference between Figs. 8a and 8d is that in the latter panel, *Jason-2* H_s values tend obviously to be higher than model estimates in the 6–10 m range, whereas this is not evident in Fig. 8a. As the correction of Ifremer waves given by Eq. (5) is only a simple approximation, this relative discrepancy is not unexpected. Figures 8b and 8e show the comparison between *HY-2* raw data and model estimates. As expected, the statistics are more scattered than that for *Jason-2*. The shaded contours show an underestimation of *HY-2* H_s values in high seas. The improvement in *HY-2* H_s values in phase 2 can be seen through better error metrics and the more compact contours in Fig. 8e. Finally, *HY-2* H_s measurements, calibrated by Eqs. (7) and (8), are compared

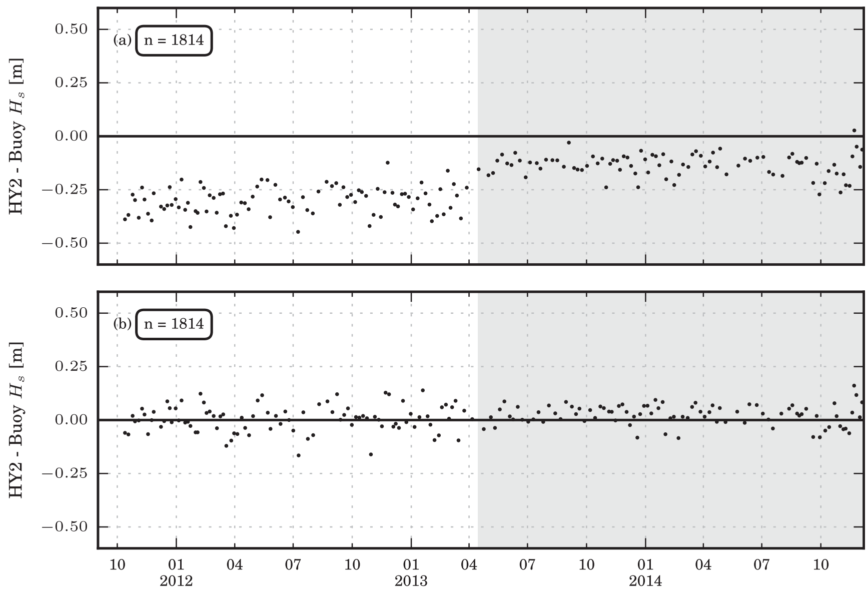

FIG. 7. As in Fig. 4, but for the difference between buoy and *HY-2* (a) raw H_s measurements and (b) calibrated H_s measurements using Eqs. (7) and (8).

with collocated model estimates in Figs. 8c and 8f. As seen in these two panels, our calibration significantly improves the performance of *HY-2* H_s values, particularly when bias is considered. Both the statistics and the patterns are much closer to those of *Jason-2* (Figs. 8a and 8d), except that *HY-2* H_s values are slightly scattered. It is worth noting that the overestimation of *HY-2* values in low sea states, which is not conspicuous in collocated measurements by *HY-2* and buoys or other altimeters (Figs. 2 and 3), now becomes noticeable. These small waves, however, were not resolved sufficiently by our quality-controlled datasets (see also section 3a) and hence no attempt was made to correct them.

6. Conclusions

The H_s values obtained by the *HY-2* altimeter (IGDRs) and three other concurrently operated satellite altimeters were evaluated against NDBC buoys. A cross validation of these four altimeters was also undertaken. From our studies, the following conclusions are drawn.

1) Among the four altimeters, *SARAL* gives the lowest RMSE (0.13 m) and the lowest scatter index (0.07), followed by *Jason-2*, *CryoSat-2*, and *HY-2*. Despite this, *HY-2* obtained H_s values are still well within its stated accuracy (Fig. 2).
2) When compared with in situ buoy measurements, *HY-2* H_s values have a tendency to underestimate real sea states when $H_s > 1$ m (Fig. 2a) and overestimate small waves (Figs. 8c and 8f). However, this latter characteristic is not well resolved by our quality-controlled datasets, in which a severe dearth of small waves exists. The absence of the ''good'' small waves in *HY-2* H_s estimates probably resulted from the error in the data retrieval algorithm, as

TABLE 3. The final calibrations of H_s from each altimeter used in our work. Statistical parameters are for the calibrated data, relative to buoys.

Altimeter	Period	Calibration	b (m)	ρ	ε (m)	ε^* (m)	N
Jason-2	25 Sep 2011–19 Oct 2014	$H_s^* = 1.019 \times H_s - 0.050$	0.02	0.99	0.14	0.14	3164
CryoSat-2	29 Sep 2011–4 Dec 2014	$H_s^* = \begin{cases} 0.836 \times H_s + 0.157 & H_s \le 1.853\,\text{m} \\ 1.001 \times H_s - 0.149 & H_s > 1.853\,\text{m} \end{cases}$	0.10	0.99	0.19	0.14	2820
HY-2	1 Oct 2011–1 Apr 2013	$H_s^* = \begin{cases} 1.003 \times H_s + 0.287 & H_s \le 3.504\,\text{m} \\ 0.040 \times H_s^2 + 0.838 \times H_s + 0.376 & H_s > 3.504\,\text{m} \end{cases}$	−0.31	0.98	0.37	0.19	932
HY-2	15 Apr 2013–6 Dec 2014	$H_s^* = \begin{cases} 0.977 \times H_s + 0.187 & H_s \le 3.568\,\text{m} \\ 0.013 \times H_s^2 + 1.083 \times H_s - 0.359 & H_s > 3.568\,\text{m} \end{cases}$	−0.13	0.98	0.21	0.16	882
SARAL	14 Mar 2013–30 Oct 2014	$H_s^* = 0.997 \times H_s - 0.056$	0.06	0.99	0.13	0.11	1657

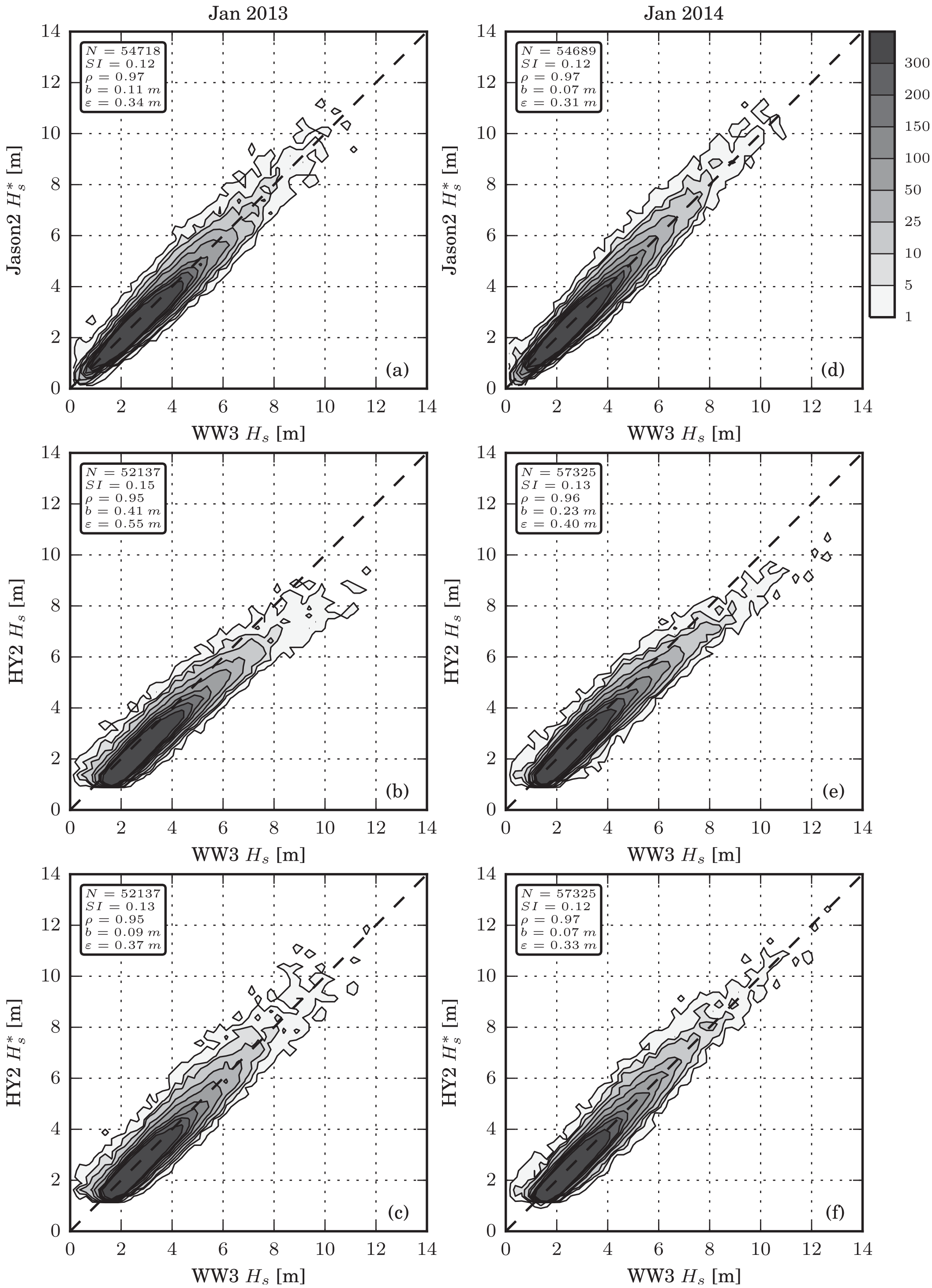

FIG. 8. Comparison between (top) *Jason-2* H_s, *HY-2* (middle) H_s, and (bottom) H_s^*vs Ifremer wave hindcast products for January (a)–(c) 2013 and (d)–(f) 2014. The model H_s values were corrected by Eq. (5). The H_s values on the vertical axes represent raw data, while H_s^* represents values calibrated by formulas summarized in Table 3.

pointed out in Zhang et al. (2015). The underestimation of *HY-2* H_s values becomes more marked for a high sea state ($H_s > 6$ m), contributing to the mismatch between the *HY-2* and other altimeters (Fig. 3). Furthermore, influenced by the switch to backup status of *HY-2* sensors and the subsequent update of data processing software, *HY-2* altimeter-measured H_s values moved to a better quality level in April 2013 and afterward (corresponding to cycle $\geq$ 41), and approached the accuracy of *CryoSat-2* wave products.

3) We finally proposed a two-branched calibration for *HY-2-* and *CryoSat-2*-estimated H_s values. The whole duration of *HY-2*, considered in our study, was subdivided into two phases on the basis of their different performances during these two periods. A detailed summary of the calibrations of the four altimeters can be seen in Table 3. These calibrations behave in a significantly consistent way. The best agreement is found between *Jason-2* and *SARAL* values (Figs. 3 and 4). Inspection of Table 3 (column ε^*) shows that determining significant wave heights using *HY-2* H_s measurements is eventually enhanced and is comparable with the other three satellite missions.
4) Our calibration for *HY-2* H_s values was further verified in an indirect way by using outputs from a wave model. When compared to the model, *HY-2* obtained H_s values present similar patterns and statistics to those from *Jason-2*; thus indicating that *HY-2* derived wave products, once calibrated, are as realistic as those from *Jason-2*.

As mentioned in section 1, NSOAS is now reprocessing *HY-2* altimeter IGDRs by adopting a different retracking method with the objective to supply a much better sea surface height (h) and wind speed U_{10}. The reprocessed data, as demonstrated in Zhang et al. (2015), also have a marginal improvement in wave height values. Our results presented here summarize and complement the existing studies on the calibration of *HY-2* H_s values, confirm its good quality, enhance its practicability especially for extreme weather research, and point out the potential deficiencies to be further improved by new data. For completeness, the assessment of the *HY-2* altimeter-derived U_{10} values will be reported in the future.

The study focused on the ability of satellite-altimeters to derive H_s in open water. Buoys less than 40 km offshore were not considered in order to eliminate land contamination. As shown in Zieger et al. (2009), with the development of satellite altimetry, wave products derived from data obtained by these altimeters in the last two to three decades are fairly reliable; however, the performance of measurements of this kind in coastal areas was limited until the recent advent of *SARAL* (Hithin et al. 2015). The use of the Ka band enables *SARAL* to yield more precise estimates of waves in coastal waters. This advancement might have many practical implications, and at the very least can be used to validate and improve the skills of numerical wave models near the coast. As stated in Sepùlveda et al. (2015), good coastal measurements can be used to study fetch-limited wind-wave growth in finite depth water. However, the difficulty in finding regions suitable for this objective might hinder its feasibility.

Acknowledgments. Q. Liu acknowledges the fellowship supported by the China Scholarship Council (CSC). Radar altimeter data were kindly provided by NSOAS, AVISO, and NOAA/NESDIS. The in situ buoy observations were provided by NDBC and NODC. The wave model output provided by the Ifremer IOWAGA project is highly acknowledged. C. Guan and J. Sun appreciate the support from the National Natural Science Foundation of China (Grants 41276010, 41376010 and U1406401). AVB acknowledges support from the Australian Research Council Discovery Grant DP130100227 and the U.S. Office of Naval Research Grant N00014-13-1-0278. We would like to thank the two anonymous reviewers and the editor for their comments and suggestions that have improved this paper.

REFERENCES

Abdalla, S., 2012: Ku-band radar altimeter surface wind speed algorithm. *Mar. Geod.*, **35**, 276–298, doi:10.1080/01490419.2012.718676.

——, and H. Hersbach, 2004: The technical support for global validation of ERS wind and wave products at ECMWF. European Space Agency Contract Rep., Final Rep. for European Space Agency Contract 15988/02/I-LG, ECMWF, 46 pp.

Ardhuin, F., and Coauthors, 2010: Semiempirical dissipation source functions for ocean waves. Part I: Definition, calibration, and validation. *J. Phys. Oceanogr.*, **40**, 1917–1941, doi:10.1175/2010JPO4324.1.

——, J. Tournadre, P. Queffeulou, F. Girard-Ardhuin, and F. Collard, 2011: Observation and parameterization of small icebergs: Drifting breakwaters in the southern ocean. *Ocean Modell.*, **39**, 405–410, doi:10.1016/j.ocemod.2011.03.004.

Ash, E., 2010: DUE GlobWave product user guide. Deliverable D5, European Space Agency Product User Guide, GlobWave Doc. GlobWave/DD/PUG Issue 1.4, 73 pp. [Available online at http://globwave.ifremer.fr/download/GlobWave_D.5_PUG_v1.2.pdf.]

Babanin, A. V., and V. K. Makin, 2008: Effects of wind trend and gustiness on the sea drag: Lake George study. *J. Geophys. Res.*, **113**, C02015, doi:10.1029/2007JC004233.

——, K. N. Tsagareli, I. R. Young, and D. J. Walker, 2010: Numerical investigation of spectral evolution of wind waves. Part II: Dissipation term and evolution tests. *J. Phys. Oceanogr.*, **40**, 667–683, doi:10.1175/2009JPO4370.1.

——, S. Zieger, and A. Ribal, 2014: Satellite observations of waves in the Arctic Ocean. *Proceedings of the 22nd IAHR International Symposium on Ice*, IAHR, 798–805.

Badulin, S., 2014: A physical model of sea wave period from altimeter data. *J. Geophys. Res. Oceans*, **119**, 856–869, doi:10.1002/2013JC009336.

Bidlot, J.-R., D. J. Holmes, P. A. Wittmann, R. Lalbeharry, and H. S. Chen, 2002: Intercomparison of the performance of operational ocean wave forecasting systems with buoy data. *Wea. Forecasting*, **17**, 287–310, doi:10.1175/1520-0434(2002)017<0287:IOTPOO>2.0.CO;2.

Bronner, E., A. Guillot, and N. Picot, 2013: SARAL/Altika Products Handbook. User Guide, CNES Doc. SALP-MU-M-OP-15984-CN, EUMETSAT Doc. EUM/OPS-JAS/MAN/08/0041, 76 pp. [Available online at http://www.aviso.altimetry.fr/fileadmin/documents/data/tools/SARAL_Altika_products_handbook.pdf.]

Caires, S., and A. Sterl, 2003: Validation of ocean wind and wave data using triple collocation. *J. Geophys. Res.*, **108**, 3098, doi:10.1029/2002JC001491.

——, ——, J.-R. Bidlot, N. Graham, and V. Swail, 2004: Intercomparison of different wind–wave reanalyses. *J. Climate*, **17**, 1893–1913, doi:10.1175/1520-0442(2004)017<1893:IODWR>2.0.CO;2.

Cavaleri, L., and Coauthors, 2007: Wave modelling—The state of the art. *Prog. Oceanogr.*, **75**, 603–674, doi:10.1016/j.pocean.2007.05.005.

Chawla, A., D. M. Spindler, and H. L. Tolman, 2013: Validation of a thirty year wave hindcast using the Climate Forecast System Reanalysis winds. *Ocean Modell.*, **70**, 189–206, doi:10.1016/j.ocemod.2012.07.005.

Chelton, D. B., J. C. Ries, B. J. Haines, L.-L. Fu, and P. S. Callahan, 2001: Satellite altimetry. *Satellite Altimetry and Earth Sciences: A Handbook of Techniques and Applications*, L.-L. Fu and A. Cazenave, Eds., International Geophysics Series, Vol. 69, Academic Press, 1–132.

Chen, C., J. Zhu, M. Lin, Y. Zhao, X. Huang, H. Wang, Y. Zhang, and H. Peng, 2013: The validation of the significant wave height product of HY-2 altimeter-primary results. *Acta Oceanol. Sin.*, **32**, 82–86, doi:10.1007/s13131-013-0381-6.

Chen, G., B. Chapron, R. Ezraty, and D. Vandemark, 2002: A global view of swell and wind sea climate in the ocean by satellite altimeter and scatterometer. *J. Atmos. Oceanic Technol.*, **19**, 1849–1859, doi:10.1175/1520-0426(2002)019<1849:AGVOSA>2.0.CO;2.

Cotton, P. D., D. J. T. Carter, and P. G. Challenor, 2003: Geophysical validation and cross calibration of ENVISAT RA-2 wind wave products at Satellite Observing Systems and Southampton Oceanography Centre. European Space Agency Contract Rep., 51 pp.

Donelan, M. A., 1999: Wind-induced growth and attenuation of laboratory waves. *Wind-over-Wave Couplings: Perspective and Prospects*, S. G. Sajjadi, N. H. Thomas, and J. C. R. Hunt, Eds., Institute of Mathematics and its Applications Conference Series, Vol. 69, Oxford University Press, 183–194.

——, A. V. Babanin, I. R. Young, and M. L. Banner, 2006: Wave-follower field measurements of the wind-input spectral function. Part II: Parameterization of the wind input. *J. Phys. Oceanogr.*, **36**, 1672–1689, doi:10.1175/JPO2933.1.

Dumont, J. P., V. Rosmorduc, N. Picot, E. Bronner, S. Desai, and H. Bonekamp, 2011: OSTM/Jason-2 products handbook. User Guide, CNES Doc. SALP-MU-M-OP-15815-CN, EUMETSAT Doc. EUM/OPS-JAS/MAN/08/0041, JPL Doc. OSTM-29-1237, NOAA/NESDIS Doc. Polar Series/OSTM J400, 63 pp. [Available online at http://www.ospo.noaa.gov/Products/documents/J2_handbook_v1-8_no_rev.pdf.]

Durrant, T. H., D. J. M. Greenslade, and I. Simmonds, 2009: Validation of *Jason-1* and *Envisat* remotely sensed wave heights. *J. Atmos. Oceanic Technol.*, **26**, 123–134, doi:10.1175/2008JTECHO598.1.

ESRIN/MSSL, 2012: CryoSat product handbook. European Space Agency User Guide, 90 pp. [Available online at http://emits.sso.esa.int/emits-doc/ESRIN/7158/CryoSat-PHB-17apr2012.pdf.]

Filipot, J.-F., and F. Ardhuin, 2012: A unified spectral parameterization for wave breaking: From the deep ocean to the surf zone. *J. Geophys. Res.*, **117**, C00J08, doi:10.1029/2011JC007784.

Gommenginger, C. P., M. A. Srokosz, P. G. Challenor, and P. D. Cotton, 2003: Measuring ocean wave period with satellite altimeters: A simple empirical model. *Geophys. Res. Lett.*, **30**, 2150, doi:10.1029/2003GL017743.

Gourrion, J., D. C. Vandemark, S. Bailey, B. Chapron, G. P. Gommenginger, P. G. Challenor, and M. A. Srokosz, 2002: A two-parameter wind speed algorithm for Ku-band altimeters. *J. Atmos. Oceanic Technol.*, **19**, 2030–2048, doi:10.1175/1520-0426(2002)019<2030:ATPWSA>2.0.CO;2.

Greenslade, D. J. M., and I. R. Young, 2004: A validation of ERS-2 fast delivery significant wave height. BMRC Research Rep. 97, 23 pp.

Hanafin, J. A., and Coauthors, 2012: Phenomenal sea states and swell from a North Atlantic storm in February 2011: A comprehensive analysis. *Bull. Amer. Meteor. Soc.*, **93**, 1825–1832, doi:10.1175/BAMS-D-11-00128.1.

Hithin, N. K., P. G. Remya, T. M. Balakrishnan Nair, R. Harikumar, R. Kumar, and S. Nayak, 2015: Validation and intercomparison of SARAL/AltiKa and PISTACH-derived coastal wave heights using in-situ measurements. *IEEE J. Sel. Top. Appl. Earth Obs. Remote Sens.*, 4120–4129, doi:10.1109/JSTARS.2015.2418251.

Janssen, P., 2004: *The Interaction of Ocean Waves and Wind*. Cambridge University Press, 300 pp.

Jia, Y., Y. Zhang, and M. Lin, 2014: Verification of HY-2 satellite radar altimeter wind retrieval. *Eng. Sci.*, **2014** (6), 54–59.

Kim, M. C., 1997: Theory of satellite ground-track crossovers. *J. Geod.*, **71**, 749–767, doi:10.1007/s001900050141.

Leckler, F., F. Ardhuin, J. F. Filipot, and A. Mironov, 2013: Dissipation source terms and whitecap statistics. *Ocean Modell.*, **70**, 62–74, doi:10.1016/j.ocemod.2013.03.007.

Li, J.-G., and A. Saulter, 2014: Unified global and regional wave model on a multi-resolution grid. *Ocean Dyn.*, **64**, 1657–1670, doi:10.1007/s10236-014-0774-x.

Lillibridge, J., R. Scharroo, S. Abdalla, and D. Vandemark, 2014: One- and two-dimensional wind speed models for Ka-band altimetry. *J. Atmos. Oceanic Technol.*, **31**, 630–638, doi:10.1175/JTECH-D-13-00167.1.

Lionello, P., H. Günther, and P. A. E. M. Janssen, 1992: Assimilation of altimeter data in a global third-generation wave model. *J. Geophys. Res.*, **97**, 14 453, doi:10.1029/92JC01055.

Mackay, E. B. L., C. H. Retzler, P. G. Challenor, and C. P. Gommenginger, 2008: A parametric model for ocean wave period from K_u band altimeter data. *J. Geophys. Res.*, **113**, C03029, doi:10.1029/2007JC004438.

Monaldo, F., 1988: Expected differences between buoy and radar altimeter estimates of wind speed and significant wave height and their implications on buoy-altimeter comparisons. *J. Geophys. Res.*, **93**, 2285–2302 pp., doi:10.1029/JC093iC03p02285.

NSOAS, 2013: HY-2A satellite user guide. National Satellite Ocean Application Service, 10 pp. [Available online at http://www.nsoas.gov.cn/.]

Queffeulou, P., 2004: Long-term validation of wave height measurements from altimeters. *Mar. Geod.*, **27**, 495–510, doi:10.1080/01490410490883478.

——, 2013a: Cryosat-2 IGDR SWH assessment update. Tech. Rep., Laboratoire d'Océanographie Spatiale, Ifremer, 12 pp. [Available online at ftp://ftp.ifremer.fr/ifremer/cersat/products/swath/altimeters/waves/documentation/cryosat_2_igdr_swh_assessment_update.pdf.]

——, 2013b: Merged altimeter wave height data base. An update. *Proceedings of ESA Living Planet Symposium*, L. Ouwehand, Ed., European Space Agency SP-722. [Available online at http://www.livingplanet2013.org/abstracts/851822.htm.]

——, and D. Croizé-Fillon, 2016: Global altimeter SWH data set. User Guide, Laboratoire d'Océanographie Spatiale, Ifremer, 10 pp. [Available online at ftp://ftp.ifremer.fr/ifremer/cersat/products/swath/altimeters/waves/documentation/altimeter_wave_merge__11.2.pdf.]

——, F. Ardhuin, and J.-M. Lefèvre, 2011: Wave height measurements from altimeters: Validation status and applications. *Proc. OSTST 2011 Meeting*, San Diego, CA, AVISO. [Available online at http://www.aviso.altimetry.fr/fileadmin/documents/OSTST/2011/poster/Queffeulou_posterOSTST.pdf.]

Rascle, N., and F. Ardhuin, 2013: A global wave parameter database for geophysical applications. Part 2: Model validation with improved source term parameterization. *Ocean Modell.*, **70**, 174–188, doi:10.1016/j.ocemod.2012.12.001.

——, ——, P. Queffeulou, and D. Croizé-Fillon, 2008: A global wave parameter database for geophysical applications. Part 1: Wave-current–turbulence interaction parameters for the open ocean based on traditional parameterizations. *Ocean Modell.*, **25**, 154–171, doi:10.1016/j.ocemod.2008.07.006.

Ray, R. D., and B. D. Beckley, 2012: Calibration of ocean wave measurements by the TOPEX, *Jason-1*, and *Jason-2* satellites. *Mar. Geod.*, **35** (Suppl.), 238–257, doi:10.1080/01490419.2012.718611.

Raynal, M., 2014: HY-2A: Global statistical assessment and cross-calibration with Jason-2 over ocean. Issue 1, Tech. Rep., SALP Doc. SALP-NT-EA-22364-CLS, CLS Doc. CLS-DOS-NT-14-148, CNES, 18 pp.

Rinne, E., and H. Skourup, 2012: Sea ice detection using EnviSat Radar Altimeter 2. *2012 Fall Meeting*, San Francisco, CA, Amer. Geophys. Union, Abstract C21C-0618.

Rogers, W. E., A. V. Babanin, and D. W. Wang, 2012: Observation-consistent input and whitecapping dissipation in a model for wind-generated surface waves: Description and simple calculations. *J. Atmos. Oceanic Technol.*, **29**, 1329–1346, doi:10.1175/JTECH-D-11-00092.1.

Sepùlveda, H. H., P. Queffeulou, and F. Ardhuin, 2015: Assessment of SARAL AltiKa wave height measurements relative to buoy, Jason-2 and Cryosat-2 data. *Mar. Geod.*, **38** (Suppl.), 449–465, doi:10.1080/01490419.2014.1000470.

Smith, T. A., and Coauthors, 2013: Ocean–wave coupled modeling in COAMPS-TC: A study of Hurricane Ivan (2004). *Ocean Modell.*, **69**, 181–194, doi:10.1016/j.ocemod.2013.06.003.

Stopa, J. E., and K. F. Cheung, 2014: Intercomparison of wind and wave data from the ECMWF Reanalysis Interim and the NCEP Climate Forecast System Reanalysis. *Ocean Modell.*, **75**, 65–83, doi:10.1016/j.ocemod.2013.12.006.

Tolman, H. L., 2002: Validation of WAVEWATCH III version 1.15 for a global domain. NOAA/NWS/NCEP/OMB Tech. Note 213, 37 pp. [Available online at http://polar.ncep.noaa.gov/mmab/papers/tn213/OMB_213.pdf.]

——, J.-H. G. M. Alves, and Y. Y. Chao, 2005: Operational forecasting of wind-generated waves by Hurricane Isabel at NCEP. *Wea. Forecasting*, **20**, 544–557, doi:10.1175/WAF852.1.

——, M. L. Banner, and J. M. Kaihatu, 2013: The NOPP operational wave model improvement project. *Ocean Modell.*, **70**, 2–10, doi:10.1016/j.ocemod.2012.11.011.

Tournadre, J., K. Whitmer, and F. Girard-Ardhuin, 2008: Iceberg detection in open water by altimeter waveform analysis. *J. Geophys. Res.*, **113**, C08040, doi:10.1029/2007JC004587.

Tran, N., F. Girard-Ardhuin, R. Ezraty, H. Feng, and P. Féménias, 2009: Defining a sea ice flag for Envisat altimetry mission. *IEEE Geosci. Remote Sens. Lett.*, **6**, 77–81, doi:10.1109/LGRS.2008.2005275.

Wang, J., J. Zhang, and J. Yang, 2013: The validation of HY-2 altimeter measurements of a significant wave height based on buoy data. *Acta Oceanol. Sin.*, **32**, 87–90, doi:10.1007/s13131-013-0382-5.

Yang, J., G. Xu, Y. Xu, and X. Chen, 2014: Calibration of significant wave height from HY-2A satellite altimeter. *Remote Sensing and Modeling of Ecosystems for Sustainability XI*, W. Gao, N.-B. Chang, and J. Wang, Eds., International Society for Optical Engineering (SPIE Proceedings, Vol. 9221), 92210B, doi:10.1117/12.2060607.

Ye, X., M. Lin, and Y. Xu, 2015: Validation of Chinese HY-2 satellite radar altimeter significant wave height. *Acta Oceanol. Sin.*, **34**, 60–67, doi:10.1007/s13131-015-0667-y.

Young, I. R., 1999: *Wind Generated Ocean Waves*. Elsevier Ocean Engineering Series, Vol. 2, Elsevier, 288 pp.

——, and G. J. Holland, 1996: *Atlas of the Oceans: Wind and Wave Climate*. Vol. 2. Pergamon Press, 241 pp.

——, and J. Vinoth, 2013: An ''extended fetch'' model for the spatial distribution of tropical cyclone wind–waves as observed by altimeter. *Ocean Eng.*, **70**, 14–24, doi:10.1016/j.oceaneng.2013.05.015.

——, S. Zieger, and A. V. Babanin, 2011: Global trends in wind speed and wave height. *Science*, **332**, 451–455, doi:10.1126/science.1197219.

——, A. V. Babanin, and S. Zieger, 2013: The decay rate of ocean swell observed by altimeter. *J. Phys. Oceanogr.*, **43**, 2322–2333, doi:10.1175/JPO-D-13-083.1.

——, S. Zieger, and A. Babanin, 2015: Development and application of a global satellite database of wind and wave conditions. *Ocean Engineering*, Vol. 7, *Proceedings of the ASME 34th International Conference on Ocean, Offshore and Arctic Engineering 2015*, ASME, OMAE2015-41039, V007T06A062, doi:10.1115/OMAE2015-41039.

Zhang, H., Q. Wu, and G. Chen, 2015: Validation of *HY-2A* remotely sensed wave heights against buoy data and *Jason-2* altimeter measurements. *J. Atmos. Oceanic Technol.*, **32**, 1270–1280, doi:10.1175/JTECH-D-14-00194.1.

Zieger, S., 2010: Long term trends in ocean wind and wave height. Ph.D. thesis, Swinburne University of Technology, 166 pp.

——, J. Vinoth, and I. R. Young, 2009: Joint calibration of multiplatform altimeter measurements of wind speed and wave height over the past 20 years. *J. Atmos. Oceanic Technol.*, **26**, 2549–2564, doi:10.1175/2009JTECHA1303.1.

——, A. V. Babanin, and A. Ribal, 2013: Wave climate in the marginal ice zone as observed by altimeters. *2013 Fall Meeting*, San Francisco, CA, Amer. Geophys. Union, Abstract OS11B-1652.

——, ——, W. E. Rogers, and I. R. Young, 2015: Observation-based source terms in the third-generation wave model WAVEWATCH. *Ocean Modell.*, **96**, 2–25, doi:10.1016/j.ocemod.2015.07.014.